

Supporting information:

A Simultaneous Increase in the ZT and the Corresponding Critical Temperature of P-type $\text{Bi}_{0.4}\text{Sb}_{1.6}\text{Te}_3$ by a Combined Strategy of Dual Nano-inclusions and Carrier Engineering

Ye Xiao^a, Jun-you Yang^{*a}, Qing-hui Jiang^a, Liang-wei Fu^a, Yu-bo Luo^a, Ming Liu^a, Dan Zhang^a, Shu-sen Wu^a, Ming-yang Zhang^a, Wei-xin Li^a, Jiang-ying Peng^b and Fu-qiang Chen^c

^a State Key Laboratory of Material Processing and Die & Mould Technology, Huazhong University of Science and Technology, Wuhan 430074, P. R China.

^b School of Mechanical Science and Engineering, Huazhong University of Science & Technology, Wuhan 430074, P. R China.

^c State Key Laboratory of State Key Laboratory of laser propulsion & application, Equipment Academy, Beijing 101400, P. R China.

* To whom correspondence should be addressed. Email: junyou.yang@163.com

1. Formation energy and density of state calculations:

The formation energy and density of state calculations were based on the density functional theory (DFT) in generalized gradient approximations (GGA) implemented by Perdew-Burke-Ernzerhof (PBE) functional with the spin-orbit interaction, using CASTEP package provided by Materials Studio. The kinetic energy cutoff and Monkhorst-Pack K-point meshes were selected to be 380eV and $6\times 6\times 4$, respectively, for a $2\times 1\times 1$ supercell composed 30 atoms. In addition, all the calculations were followed by Geometry optimizations with the criteria: total energy, maximum force, maximum stress, maximum displacement were converged to less than 5×10^{-6} eV/atom, $0.01\text{eV}/\text{\AA}$, 0.02GPa , 5.0×10^{-4} \AA, respectively.

2. The EDAX analysis on the matrix of $\text{Bi}_{0.4}\text{Sb}_{1.6}\text{Te}_3$

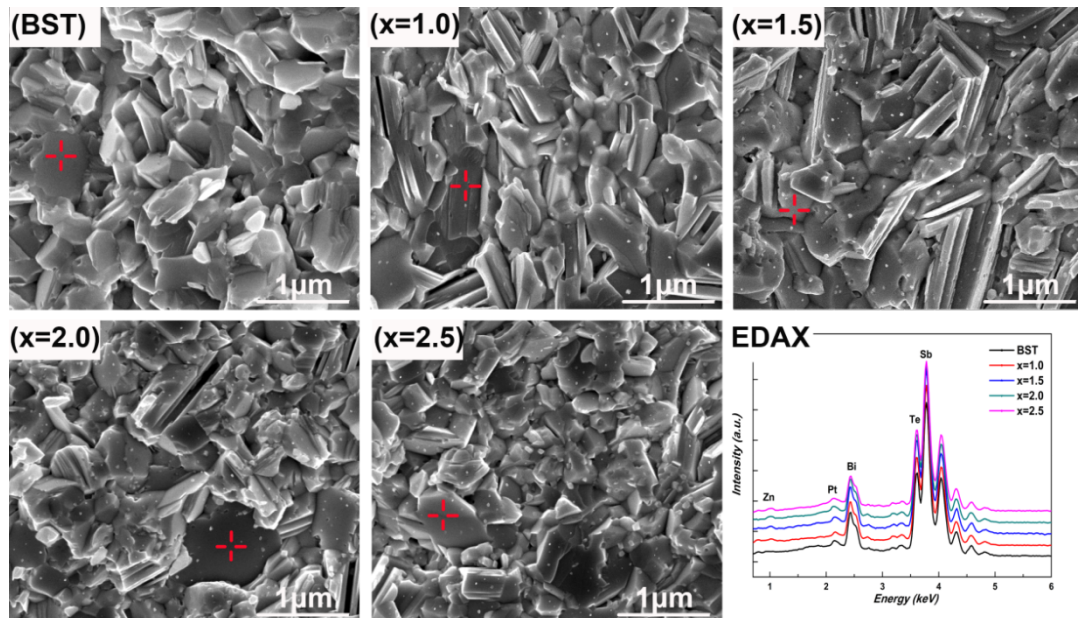


Figure S1. The EDAX analysis on the matrix of $\text{Bi}_{0.4}\text{Sb}_{1.6}\text{Te}_3$

Table 1. Elemental composition varies different amount

	Zn(atom%)	Bi(atom%)	Sb(atom%)	Te(atom%)
BST	0	7.86	32.86	59.25
X=1.0	0.63	7.78	32.69	58.90
X=1.5	1.11	7.62	32.51	58.76
X=2.0	1.28	7.58	32.49	58.65
X=2.5	1.32	7.56	32.47	58.65

3. EDAX result of the Zn nanoinclusions in the Figure 4b.

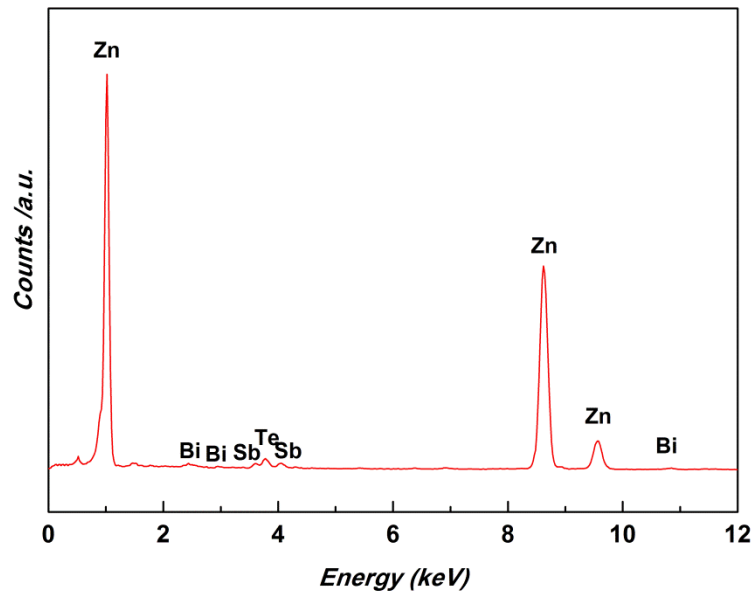


Figure S2. Corresponding EDAX result in Figure 4b

4. Power factors of the samples with different content of β -Zn₄Sb₃:

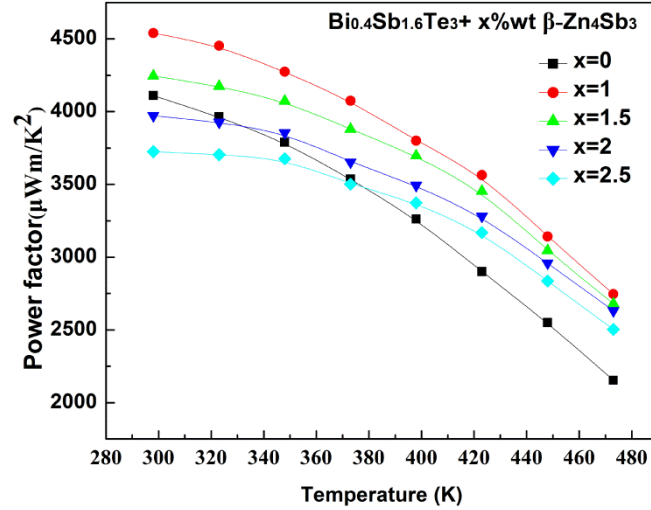


Figure S3. Power factors as a function of temperature for $\text{Bi}_{0.4}\text{Sb}_{1.6}\text{Te}_3 + x\% \text{wt } \beta\text{-Zn}_4\text{Sb}_3$

5. Estimation of κ_{ph} and κ_{bp} :

Kitagawa et al¹ proposed a simple method to estimate the contribution of bipolar conduction to total thermal conductivity at high temperature. Firstly, we can get $\kappa_{\text{tot}} - \kappa_{\text{e}}$ by Wiedemann–Franz law ($L=2.00 \times 10^{-8} \text{ V}^2 \text{ K}^{-2}$). As suggested by Slack³, the lattice thermal conductivity should follow the relationship $\kappa_{\text{ph}} \sim T^{-1}$. In our case, the $\kappa_{\text{tot}} - \kappa_{\text{e}}$ (Figure S3) follows that linear relationship with T^{-1} at low temperature quite well but it begins to deviate at high temperature which relates to bipolar excitation temperature. The κ_{ph} at high temperature is estimated by extrapolating the linear relationship of $\kappa_{\text{ph}} \sim T^{-1}$ as shown by the dashed line in Figure S3 and the κ_{bp} can be estimated by $\kappa_{\text{tot}} - \kappa_{\text{e}} - \kappa_{\text{ph}}$. The temperature variations of κ_{bp} are shown in the inset of Figure 5c and the κ_{ph} in Figure 5d respectively.

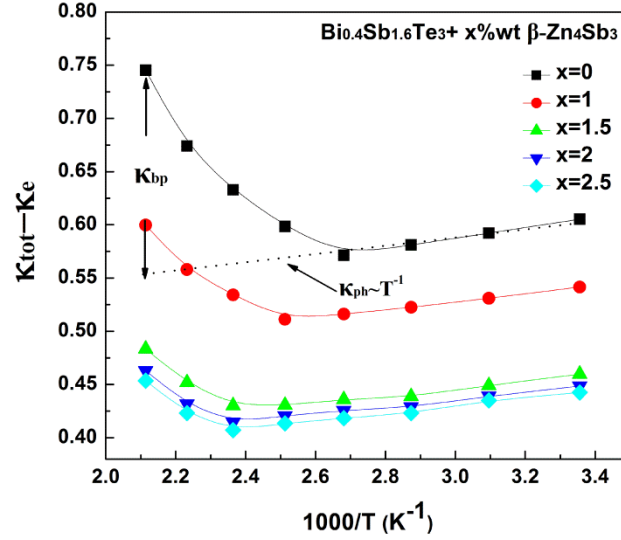


Figure S4. Total thermal conductivity minus electron thermal conductivities as a function of temperature for $\text{Bi}_{0.4}\text{Sb}_{1.6}\text{Te}_3 + x\% \text{wt } \beta\text{-Zn}_4\text{Sb}_3$

6. Estimation of the relaxation times:

The relaxation time of Umklapp processes which were introduced by Slack³ is expressed as:

$$\tau_U^{-1} = \frac{\hbar \gamma^2 \omega^2 T}{M c^2 \theta_D} e^{-\theta_D/3T}$$

where M is the average mass of an atom in the crystal, \hbar is reduced Plank constant, γ is the Grüneisen parameter, θ_D is the Debye temperature and c is the average phonon velocity. For our systems, $\gamma=1.6$, $\theta_D=165\text{K}$, $c=2922\text{ms/s}$, the $\omega=2.16 \times 10^{13}$ is the cut off frequency and ω_0 is the reduce phonon frequency^{4,5}.

The point defects scattering, mainly due to the isotopes and alloying atoms in the matrix can be expressed as⁴:

$$\tau_D^{-1} = \frac{\Omega}{4\pi c^3} \Gamma_i \omega^4$$

Where Ω is the volume of primitive crystal. Expressions for the isotopic and alloying contributions towards Γ_{md} , viz. Γ_{isotopes} and Γ_{alloy} are 0.025 and 0.05⁴ respectively.

The nanoparticles' contribution to the relaxation was estimated as follows⁶⁻⁹

$$\tau_{NP}^{-1} = c(\sum \sigma_i^{-1})^{-1} V_p$$

$$\sigma_s = 2\pi R^2 \quad \sigma_l = \frac{4}{9}\pi R^2 \left(\frac{\Delta D}{D}\right)^2 \left(\frac{\omega R}{c}\right)^4$$

Where V_p is the density of nanoparticles R is the average size of nanoinclusions, the subscript $i=s,l$ denotes low and high phonon frequency contributions respectively and D is the mass density of materials. The corresponding results are shown in the inset of Figure 5d.

References :

1. H. Kitagawa, M. Wakatsuki, H. Nagaoka, H. Noguchi, Y. Isoda, K. Hasezaki, and Y. Noda, *J. Phys. Chem. Solids* 66, 1635, 2005.
2. Xie WJ, Tang XF, Yan Y, Zhang Q, Tritt TM. *Appl Phys Lett* 2009;94:102111-3
3. G A Slack, *Solid State Physics* 34, 1 (1979).
4. Ö Ceyda Yelgel and G. P. Srivastava, *J Apply Phys.* 113, 073709 (2013)
5. Masayuki Takashiri, Saburo Tanaka, Harutoshi Hagino, Koji Miyazaki, *J Appl Phys.* 112, 084315 (2012)
6. C. B. Vining, *J. Appl. Phys.*, 1991, 69, 331.
7. N. Mingo, D. Hauser, N. P. Kobayashi, M. Plissonnier, A. Shakour, *Nano Ltee.*, 2009, 9, 711.
8. J. He, J. Androulakis, M. G. Kanatzidis, V. P. Dravid, *Nano Lett.*, 2012, 12, 343.
9. J. He, S. N. Girard, J. Zheng, L. Zhao, M. G. Kanatzidis, V. P. Dravid, *Adv. Mater.*, 2012, 24, 4440.